Multimodal Neuroimaging with Simultaneous fMRI and EEG

Govinda R. Poudel and Richard D. Jones

Contents

G. R. Poudel (✉)
Mary Mackillop Institute for Health Research, Faculty of Health Sciences, Australian Catholic University, Melbourne, VIC, Australia
e-mail: Govinda.poudel@acu.edu.au

R. D. Jones
New Zealand Brain Research Institute, Christchurch, New Zealand

Department of Medicine, University of Otago, Christchurch, New Zealand

Department of Electrical and Computer Engineering, University of Canterbury, Christchurch, New Zealand

School of Psychology, Speech and Hearing, University of Canterbury, Christchurch, New Zealand

N. V. Thakor (ed.), *Handbook of Neuroengineering*,
https://doi.org/10.1007/978-981-15-2848-4_81-1

Abstract

Functional magnetic resonance imaging (fMRI) and electroencephalography (EEG) are noninvasive techniques used to measure neural activity in the human brain. fMRI measures the magnetic resonance signal associated with hemodynamic changes driven by neural activity and has a good spatial resolution (2–3 mm isotropic) and low temporal resolution (1–3 s). Whereas EEG is used to record electrical activity in the brain with a millisecond-level temporal resolution but has a limited spatial resolution. By combining fMRI and EEG, it is possible to generate a high spatiotemporal resolution map of human brain function, which is critical for understanding complex dynamics of the human brain. Furthermore, EEG recordings during fMRI can be used to identify the sources of abnormal electrical activity in the brain (e.g., during epileptic seizures). This chapter discusses recent advances in the simultaneous recording of fMRI and EEG in humans. It focuses on the challenges of recording fMRI and EEG simultaneously, techniques for removing artifacts, experimental designs for fMRI and EEG studies, and methods for integrating fMRI and EEG data.

Keywords

Simultaneous EEG-fMRI · Multimodal neuroimaging · Magnetic resonance imaging · Functional magnetic resonance imaging · Concurrent EEG-fMRI · fMRI · BOLD

1 Introduction

The human is a complex and dynamic network which stores and processes information at multiple spatiotemporal scales. This information processing occurs via the generation of electrical activities in the neurons and their transmission via axonal pathways. Abnormal changes in the generation and transmission of neuroelectric activities lead to disorders of brain function. Functional magnetic resonance imaging (fMRI) and electroencephalography (EEG) can be used to noninvasively record neural activity in the brain. fMRI measures changes in the intensity of the magnetic resonance signal associated with hemodynamic changes due to neural activity. fMRI has a higher spatial resolution (2–3 mm) than EEG but suffers from limited temporal resolution (1–2 s). EEG, on the other hand, can record neural activity with a high temporal resolution (milliseconds) but has a limited spatial resolution. Simultaneous recording of fMRI and EEG can be used to combine the best of both techniques and better understand the neural sources of abnormal neuroelectric activity in the brain (e.g., during epileptic seizures) and/or generate a high spatiotemporal resolution map of human brain function [1–14].

This chapter is focused on in vivo imaging of the human brain function using simultaneous fMRI-EEG. It discusses recent advances in simultaneous fMRI and EEG based imaging of human brain function. It outlines the challenges of simultaneously recording fMRI and EEG, and techniques for removing artifacts from the EEG data recorded inside an MRI scanner. Finally, it provides technical guidelines for designing experiments to improve the utility of fMRI and EEG, and various methods for integrating fMRI and EEG data to achieve high spatial and temporal resolution.

2 Blood-Oxygen-Level-Dependent (BOLD) fMRI

Blood-oxygen-level-dependent (BOLD) fMRI was first discovered by Ogawa et al. [15] through studies of rats in a high magnetic field. An increase in neuronal activity requires greater energy (Fig. 1a), which drives a complex interaction between blood flow, oxygenated (diamagnetic) and deoxygenated (paramagnetic) blood, blood volume, and oxygen consumption [16–19]. The presence of a small additional magnetic field due to an imbalance of paramagnetic and diamagnetic blood inside an MRI scanner can generate local inhomogeneities in the magnetic field resulting in a decrease in the relaxation constant $T2^*$ of the MR signal. Thus, MR pulse sequences sensitive to $T2^*$ show more MR signal when blood is highly oxygenated and less MR signal when blood is highly deoxygenated. A typical BOLD response to a brief neuronal stimulation has a delayed onset, peak, and post-undershoot [20]. This BOLD response is known as the *hemodynamic response function* (HRF). A number of studies have also reported a brief (1–2 s) initial decrease in the HRF, known as the initial dip, following the neuronal activity and just before the rise of HRF [21, 22].

fMRI generates spatiotemporal data (Fig. 1b). The observable increase in BOLD HRF only occurs after 1–2 s of neuronal activity and peaks at about 5 s. The sampling rate in fMRI is 1–2 s. Hence, the BOLD signal is only a proxy for measuring the very fast neuronal activity which occurs at the scale of milliseconds. For the typical pulse sequence used in fMRI, one brain volume is acquired per repetition time (TR). Recent advances in multi-band fMRI allow acquisition of BOLD with sub-second level temporal resolution [23].

The spatial resolution of fMRI is determined by voxel size, which typically ranges from 2–3 mm isotropic. Smaller voxel sizes reduce the signal-to-noise ratio (SNR), whereas, very large voxels introduce low spatial specificity and partial volume effects [24]. More recent advancement in high-spatial resolution fMRI in ultra-high-field MRI scanners allows recording of fMRI at sub-millimeter spatial resolution [25]. For example, a sub-millimeter resolution fMRI can reveal laminar and columnar circuitry in humans [25]. However, difficulties associated with ultra-high-field MRIs, including the cost of scanning, limited availabilities, and safety issues, have made the regular use of these scanners impractical.

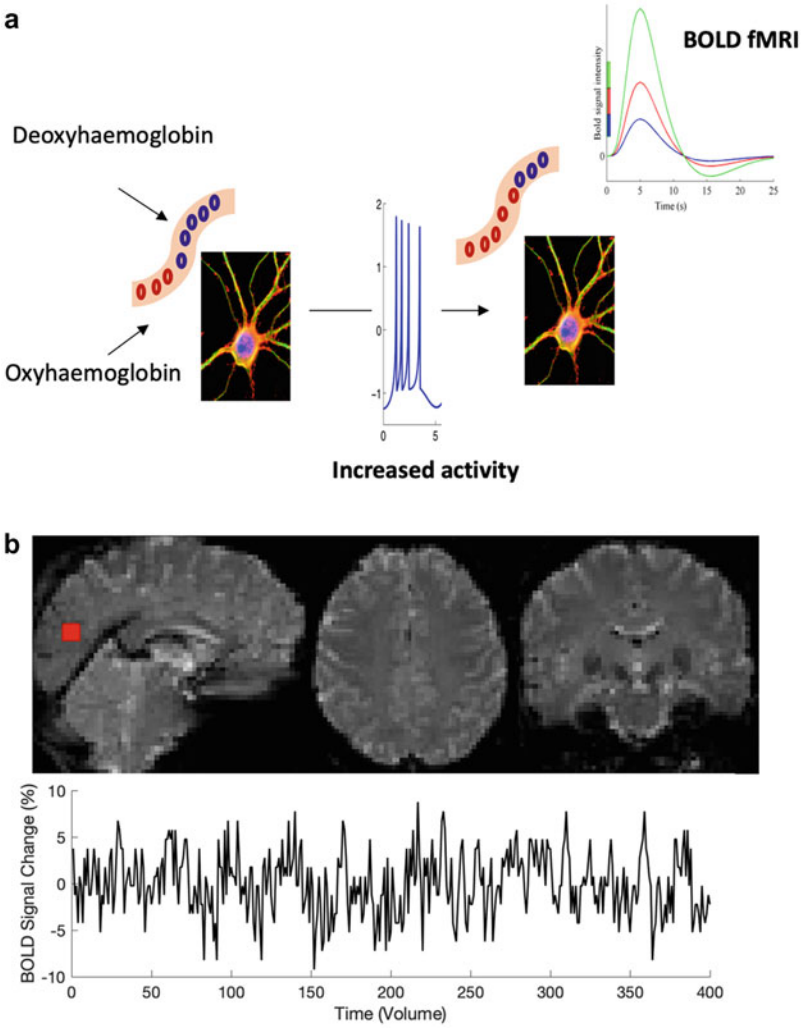

Fig. 1 Schematic showing the generation of BOLD fMRI signal. (**a**) Increased neuronal activity triggers a chemical cascade that results in elevated blood oxygenation, volume, and flow. MR pulse sequences sensitive to $T2^*$ show more MR signal when blood is highly oxygenated and less MR signal when blood is highly deoxygenated (adapted from [16]). (**b**) A typical volume and associated time-series signal from one voxel in fMRI data. Typical fMRI has a spatial resolution of 2–3 mm and temporal resolution of 1–2 s

3 Electroencephalography (EEG)

EEG measures the brain's electrical activity by placing conductive electrodes on the scalp (Fig. 2). In contrast to fMRI, EEG can capture the electrical activity with a high temporal resolution (typically in milliseconds). Hence, it is routinely

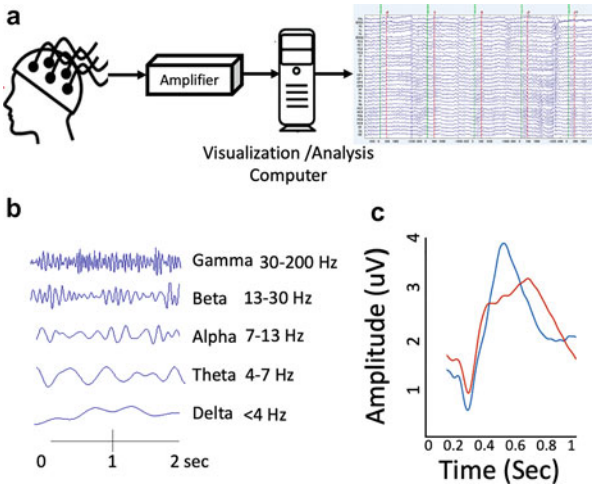

Fig. 2 EEG recording and its characteristics. (**a**) A typical EEG data acquisition setup. EEG is recorded via electrodes placed on the scalp. Data is acquired using data acquisition hardware (amplifier) and visualized and analyzed on a computer. (**b**) Different frequency bands within EEG recordings are associated with different brain states. (**c**) An example of average event-related potentials (ERPs) which are time-locked to a stimulus can also be observed in EEG data

used clinically in the diagnosis and evaluation of several neurological disorders, especially epilepsy. EEG is also the gold standard method for classifying different stages of sleep in humans. It is used routinely in the evaluation of sleep disorders, for which there are established clinical guidelines [26].

EEG measures the total synchronous electrical activity generated by a population of neurons localized in a similar spatial orientation [27]. Therefore, the origin of EEG is largely dependent on the functional and structural connectivity of the underlying neuronal population [28]. This notwithstanding, most of the EEG signal recorded on the scalp originates from cortical pyramidal neurons [28], with deep sources (subcortical areas) more likely to be missed in routine EEG recordings.

EEG waves are commonly characterized by frequency bands of <4 Hz (delta), 4–7 Hz (theta), 7–13 Hz (alpha), 13–30 Hz (beta), and >30 Hz (gamma). Delta waves are a prominent feature of deep sleep but they are also observed during high cognitive demands and in certain brain pathologies [29, 30]. Theta waves are observed during drowsiness and can appear frequently in the sleep-deprived brain [5, 14, 31, 32]. Alpha waves reflect relaxed wakefulness with eyes-closed. Beta and gamma waves are most prominent while performing cognitive tasks. Stimulus locked neuronal firing (e.g., auditory or visual stimuli) is also evident as event-related potential on EEG data.

4 Recording EEG Inside an MRI Scanner

The first recording of EEG inside an MRI scanner was reported in the early 1990s [1]. These early initiatives were largely driven by the clinical need to identify spatial sources of epileptiform activity using EEG recorded inside MRI [1]. Hence, EEG was primarily used to detect epileptic seizures, whereas fMRI was used to localize them with good spatial accuracy. Since then, advances in hardware and

software have led to an exponential increase in the use of simultaneous fMRI-EEG in cognitive and clinical neurosciences. The focus has been broadened to encompass understanding the fMRI correlates of EEG activity during relaxed wakefulness [10, 11, 33], sleep [5, 9, 34], as well as complex cognitive tasks [8, 35].

Simultaneous fMRI-EEG is technically challenging due to the harsh electromagnetic environment of MRI [2]. The magnetic field gradients in MRI scanners generate time-varying magnetic fields, which, with modern high-field MRI scanners, can be up to 200 T/m/s. When EEG electrodes are positioned inside an MRI scanner, the time-varying magnetic fields induce currents in the electrode leads. These currents appear as large gradient artifacts in the EEG. Furthermore, movement of the EEG electrodes due to patient motion or to cardiac arterial pulsation (ballistocardiogram) generates artifacts in the EEG, which are similar in amplitude to the actual EEG signal. Early simultaneous fMRI-EEG recording systems addressed these technical challenges by using MRI-compatible EEG electrodes and only triggering fMRI data acquisition after an event of interest (e.g., epileptiform spike) was identified in the EEG [1]. This allowed for a reasonable quality EEG in the absence of gradient artifacts. The first truly simultaneous fMRI-EEG system was reported in the early 2000s [2], which incorporated analog pre-processing and digital post-processing of the EEG signal to suppress MRI artifacts. They demonstrated that by adopting a proper scanning protocol and strategies for minimizing the gradient artifacts, continuous monitoring of the EEG during fMRI scanning was possible [2].

5 MR-Compatible EEG Hardware

Since the first recordings of EEG inside an MRI scanner in the early 1990s, considerable progress has been made towards optimizing the EEG hardware. The latest commercially available hardware meets safety standard for patients and reduces interactions with the static magnetic, gradient magnetic, and radiofrequency fields. This notwithstanding, a number of safety and design consideration should be taken into account while establishing an EEG recording system inside MRI (Table 1).

5.1 Safety Considerations

There are several risks associated with placing EEG electrodes on a patient's head in an MRI scanner. These include (1) localized heating of tissues near the metallic EEG electrodes, (2) electric shock, and (3) neural stimulation. Localized heating can occur when currents are induced in conductive loops when exposed to a time-varying magnetic field generated by RF or changing gradient fields. Heating can also occur when conductive loops formed from EEG placements move slightly within the scanner (due to patient movement or ballistocardiogram-/respiration-related movement) and interact with the spatially varying static magnetic field. An increase in the strength and frequency of the magnetic field increases the induced current

Table 1 Important considerations and design challenges associated with EEG recordings inside an MRI environment

Safety Considerations
• Low-impedance conduction through the patient represents a potential hazard as currents may be induced in loops placed in the time-varying gradients and RF fields, and due to body movement in the static field.
• Low-impedance loops may form as follows: exposed lead in contact with the patient; two leads in direct electrical contact; a single lead bending on itself and the current being able to flow through the insulation at RF frequencies; and failure of the EEG pre-amplifier circuit.
• A conducting loop could also form due to the capacitance between parallel leads, with the induced current flowing through the patient.
• Heating due to eddy currents induced within the electrodes and other conducting media in contact with the patient also present a potential hazard.
Design Considerations
• The first design, used extensively in the early development of MR-compatible EEG systems, comprises passive electrodes inside the MRI bore and an active magnetic-field-compatible local amplifier (headbox) placed outside the MRI scanner.
• The second design, which has been used extensively in more recent EEG + MRI studies, has the EEG amplifier placed inside the MRI bore [6, 10]. In this design, the amplifier/digitizer is shielded and placed close to the head coil. The amplifier is usually battery- or accumulator-powered, which reduces interactions with the magnetic field, minimizes imaging artifacts, and increases patient safety.
Hardware Consideration
Electrode materials: Non-ferrous electrodes.
e.g., Ag/AgCl, Au, plastic to stainless steel.
Electrode configuration: Twisted dual leads equipped with current-limiting resistors (commonly in range 5–10 kΩ for 1.5 T scanners) to avoid heating and to reduce MR-acquisition-related EEG artifacts.
Electrode gels: Water-based electrode gels.
Sampling Rate: Up to 20 kHz per channel.
Bandwidth: DC to 4 kHz.
Dynamic Range: High
Input noise: Low (<1 μV peak-to-peak).
Data transfer: Via optic fiber/carbon cable.
Amplifier system: Faraday shielded (if within the MRI scanner room).

[36]. Hence, careful consideration is required in the design of MR-compatible EEG systems to meet the required safety standards.

5.2 EEG Hardware

The interaction between the EEG hardware , the MRI environment, and patients can be minimized by careful consideration of the components used in EEG, printed circuit board (PCB) designs, the choice of integrated circuits, and the methods used for data transfer and acquisition [6, 37, 38]. Two designs have been used

extensively for acquiring EEG inside an MRI scanner. The first design places all active electronic components (e.g., amplifier and any other electronics) outside the MRI scanner [2]. The EEG electrode leads are connected to the local amplifier via a long carbon cable. The electrodes are silver-chloride-plated plastic cups. This design minimizes artifacts on the MR images, as the active electronics of the amplifier are outside the scanner. RF-induced current loops in the lead wires are also minimized by twisting dual leads [2]. A number of variations of this system, proposed by Goldman et al. [2], have been made, including the use of high-current-limiting resistors and gold electrodes [39] and having the electrode leads connected to an amplifier located outside the MRI scanner room via a long carbon fiber cable passed through a waveguide [40]. The EEG systems based on long carbon cables have been used to successfully record EEG inside a 3 T MRI scanner in studies of microsleeps [5, 14, 41, 42].

The second design places the EEG amplifier inside the MRI room [6, 10]. In this design, the amplifier/digitizer is shielded and placed close to the head coil. The amplifier is usually battery-powered, which reduces interactions with the magnetic field, minimizes imaging artifacts, and increases patient safety. To attenuate the large high-frequency gradient artifacts induced in EEG during the acquisition of the MR signal, a differential amplifier coupled to a low-pass resistor-capacitor (RC) filter (e.g., 250 Hz) is also commonly used. The digitized EEG signal is transferred to the acquisition system outside the MRI scanner via an optical fiber. In this design, EEG signal loss is minimized by placing the amplifier closer to the cap. Furthermore, the amplifier is made up of non-magnetic material which can be placed inside the scanner bore.

6 EEG + fMRI Data Acquisition Protocol

6.1 EEG Hardware Setup

The methodological considerations provided below can help improve the workflow for EEG + fMRI studies.

1. Most of the EEG hardware should be set up in the control room, although some systems also allow EEG amplifiers to be placed closer to the participant's head (i.e., at the end of the MR bore).
2. The MRI scanner needs to send slice/volume triggers (e.g., transistor-transistor logic (TTL) pulses) for detection by the EEG system. The TTL pulses are necessary to synchronize MRI slice acquisition with EEG recordings, so that onset of gradient artifacts can be located easily on the EEG data. If the triggers are too short, external hardware may be necessary to extend the trigger pulses.
3. Similarly, the EEG system needs to be connected to a stimulus computer to receive triggers for stimulus presentation.
4. Any other peripheral devices can also be synchronized to the EEG system via additional triggers.

5. The choice of sampling rate to acquire the EEG data is also critical. A sampling rate of at least 5000 Hz or more should capture the dynamic range associated with gradient artifacts so that adaptive subtraction approaches could be used to remove the artifacts during pre-processing steps.
6. The EEG recording can be AC- or DC-coupled, depending upon the requirement of the study.
7. Furthermore, EEG electrodes can be configured according to referential or bipolar configurations. A bipolar configuration was the first method of choice in the early EEG + fMRI setups. In this setup, a twisted bipolar configuration was used to substantially reduce the gradient noise [2, 11]. For bipolar configuration, the reference electrode for each electrode is the neighboring electrode. In contrast, for referential configuration, a neutral electrode is placed on the mastoid behind the earlobe or at central electrodes.

6.2 Participants Preparation

1. A proper standard operating procedure, informed consent, and regular checking are necessary to ensure that participants are comfortable inside the MRI scanner.
2. Participants should be screened for MR safety, especially for the presence of metallic implants, prior to being recruited for the study.
3. They should be asked to clean their hair with shampoo (without conditioner) and to not apply any other hair product. Application of conditioner and other hair products may form a nonconductive barrier between the scalp surface and electrodes.
4. The EEG electrode caps must be chosen according to the head size of the participant. Electrolyte gel is placed inside each electrode to ensure conductive contact with the scalp.
5. Electrodes to measure electroencephalography (ECG) or electrooculography (EOG) should also be placed using the conductive gel. Electrode impedances should be as low as possible (<10 kΩ) to ensure good quality signal. It is important to not use an excessive amount of gel, as this can cause bridging between electrodes.
6. Visual data checking is important to ensure the quality of EEG data. This should first be done outside the scanner. A simple eyes-open/eyes-closed protocol can reveal alpha waves during the eye-closures in the posterior electrodes (e.g., Oz, O1, O2).

6.3 Acquisition Methods

There are two types of acquisitions commonly used in research studies: interleaved and continuous [7, 9, 10, 43–46].

6.3.1 Interleaved Acquisition

The interleaved acquisition is used when the experimental protocol requires epochs of EEG data without gradient artifacts or when the experimental protocol requires brief intermittent periods free of MRI audio noise (e.g., during auditory experiments). In an interleaved acquisition, fMRI images are acquired in an interleaved manner, whereas the EEG is acquired continuously. Interleaved acquisition has periods of MRI silence, which can be used as a window to present auditory stimuli [45, 47, 48]. In a typical interleaved acquisition, stimuli are presented first and a window of clean EEG without gradient artifacts is acquired immediately after stimuli presentation [44, 48]. The portions of EEG during which fMRI is not acquired will still have artifacts related to arterial pulsation (ballistocardiogram (BCG)), which should be removed using artifact rejection techniques. An important limitation of this techniques is that stimuli need to be presented with a relatively long (>10 s) inter-stimulus interval, which can substantially increase the total scan time.

6.3.2 Continuous Acquisition

Continuous acquisition of EEG and fMRI is the method of choice for most clinical simultaneous fMRI-EEG studies (e.g., in epilepsy) and for research in cognitive neurosciences. In continuous acquisition, EEG and fMRI are acquired simultaneously. This is important to interrogate event-related studies and studies employing continuous tasks [5, 14, 49, 50], which require that neuronal activity is sampled continuously over time. An additional advantage of continuous acquisition is its ability to capture unpredictable events. For example, in clinical studies such as investigations of the epileptic activity or sleep stages, the events of interest are unpredictable. Hence, fMRI and EEG are acquired continuously and events of interest in EEG are identified post-hoc [14, 51, 52]. A limitation of continuous acquisition is that large gradient artifacts inundate the EEG signal of interest. Hence, to avoid saturation during fMRI acquisition, it is important to have EEG amplifiers with a large dynamic range. Novel algorithms have been developed to remove both gradient and BCG artifacts from EEG data [53], which is discussed in the following sections.

6.4 Artifact Removal Techniques

6.4.1 Gradient Artifact

MRI scanners use time-varying magnetic fields generated by gradient and RF coils to encode spatial information from the MR signal and create an image [1–3, 10, 45]. Hence, when EEG hardware (electrodes, wires, and an amplification system) is placed inside an MRI scanner, the time-varying electromagnetic fields generate spurious voltage signals (gradient artifacts) within the conductive loops formed by the subject's head and the EEG hardware. The gradient artifacts are very large (>100 times) in amplitude compared to the neurophysiological EEG signal. There are several approaches to reduce gradient artifacts. These methods can broadly be

grouped into: (1) subtraction-based denoising, (2) blind-noise separation, and (3) hardware-based techniques.

Subtraction-Based Denoising

This method , proposed by Allen et al. [54], calculates an average imaging artifact template from a fixed number of samples, which is then subtracted from the EEG signal for each sample. The subtraction method involves the following steps [11, 39, 54, 55]:

1. The low-frequency fluctuations are removed from the EEG data (using a high pass filter at 1 Hz).
2. An average template of gradient artifacts is created by averaging artifactual signals across multiple slices or volumes.
3. The artifact template is subtracted from the signal to remove the large gradient artifacts.
4. The residual noise is removed by using adaptive noise cancelation techniques.

A prerequisite for the adaptive artifact subtraction (AAS) approach to work correctly is that the artifact template must be accurately computed. To create an accurate artifact template, it is important that synchronization between the EEG and fMRI acquisitions is precise [56, 57]. Any temporal jitters in synchronization will make the method unusable. The templates can be created by using either imaging slices or volumes. The time periods during which fMRI scans occur, based on the trigger observed on EEG data, are used for creating the template. The best results can be obtained by combining both slice- and volume-based approaches [58, 59]. Hence, it is important that slice triggers for each imaging slice are sent to the EEG system.

The second important consideration for subtraction-based removal is the residual noise after the first-pass removal. Since average template subtraction is a linear method, any nonlinear and stochastic noise will persist in the EEG data. To remove this residual noise, an eigenvalue-decomposition-based approach has been developed [56]. The method involves principal component analysis (PCA) based decomposition of the residual signal. The components which explain the most variance related to the residual noise can then be regressed out using an adaptive noise cancelation (ANC) filter [56]. An alternative approach is to apply PCA directly on the EEG data and separate noise components from signal [55]. However, this approach also requires an ANC filter to remove the residual noise. A third approach uses iterative subtraction in which the amplitude of gradient templates are optimally adjusted by linear regression [60].

To capture and remove motion-related variance in artifact templates, methods based on weighting, clustering, and regression have been proposed [57, 61, 62]. The artifact templates can be adapted to motion-related noise by weighting each occurrence based on its temporal or spectral similarity [57, 61]. Furthermore, clustering-based approaches can cluster the artifacts based on a similarity measure between the artifact template calculated for each cluster. Other approaches, based

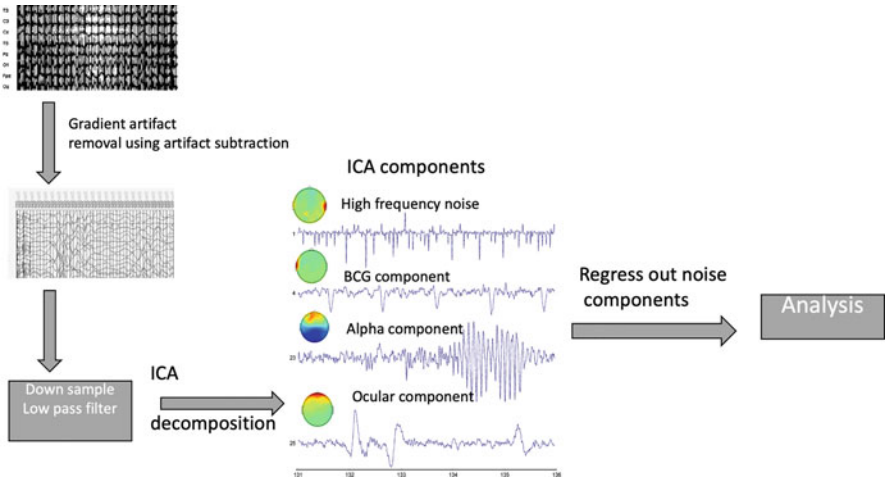

Fig. 3 High-level overview of the pipeline used for removing gradient (GA) and ballistocardiogram (BCG) artifacts from EEG data

on head-motion estimation from fMRI time-series, have also been proposed and applied [63].

Blind-Source Separation of Gradient Artifact

Blind-source separation techniques, such as independent component analysis (ICA), have been used to successfully extract noise contaminations from EEG data [6, 40, 43, 64, 65].

ICA seeks to separate N mutually statistically independent source signals from M linearly combined source signals [66]. ICA can be applied on raw EEG data to separate EEG into signal and noise sources [41]. Noise components can then be removed from signal by component regression [65]. Automated techniques, which use supervised learning to identify artifacts-related signal by identifying independent components (ICs) similar to the artifact template, may also be useful in the identification of imaging artifacts in EEG recording from inside an MRI scanner [67, 68] (Fig. 3).

Hardware-Based Approaches

Hardware-based approaches use an additional hardware component to capture, characterize, and remove gradient artifacts from EEG data [58, 69–71]. In one technique, a separate layer of EEG electrodes is placed on the top as a reference layer [69]. The electrodes below the reference layer are attached to the scalp via electrode gel [69]. These electrodes record brain signals along with gradient and motion artifacts, whereas the electrodes in the reference layer are isolated from the scalp and only record MRI artifacts [69]. The artifact-free EEG signal is then

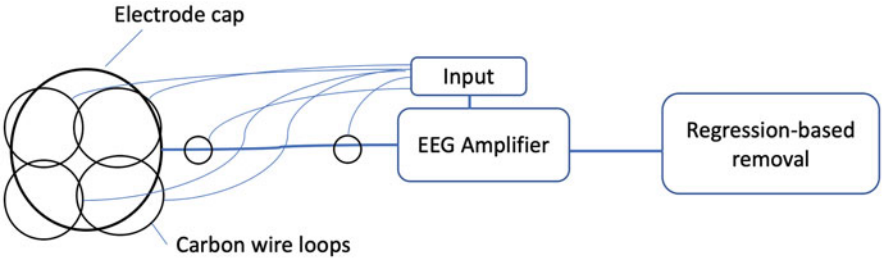

Fig. 4 Configuration of carbon-wire loop [71] developed for hardware-based removal of MR artifacts. (Adapted from [71])

estimated by removing the artifact signal (recorded via the new reference electrodes) from the cumulative EEG and artifact signal (recorded via the scalp electrode).

In another approach called the "carbon-wire loops" approach, four carbon-wire loops are stitched on the outer surface of the EEG cap together with two carbon-wire loops that are placed on the cables from the EEG cap to the EEG amplifier [71, 72] (Fig. 4). The four carbon wires have an internal resistance of 160 Ω/m and are placed on the left-frontal, left-posterior, right-frontal, and right-posterior locations [71]. The noise signals recorded by these carbon wires are then regressed out from the brain signal recorded by the EEG cap. This method has been shown to be suitable for removing any movement-related artifacts, as well as pulse, and gradient artifacts [71].

6.4.2 Ballistocardiogram (BCG) Artifacts

Ballistocardiogram (BCG) artifacts are difficult to remove dynamic artifacts on EEG generated due to (1) spurious voltages on the scalp electrodes when pulsatile motion expands or contracts the scalp in the strong magnetic field of the MRI scanner [73], (2) small head movements due to bulk movement of arterial blood [44], and (3) the Hall effect due to pulsatile motion of conductive blood. Even a small motion of EEG electrodes due to pulsatile motion can translate into an electric signal which can be several times larger than the EEG signal of interest. BCG artifacts are difficult to completely remove from EEG data due to their non-stationary nature [69, 70, 74] because of the temporal variability of the cardiac pulse.

Adaptive Subtraction of BCG Artifacts

BCG artifacts can be removed by using adaptive noise cancelation techniques [39, 54, 56]. Due to the periodic nature of BCG artifacts that are time-locked to the cardiac cycle, an adaptative average subtraction technique can be applied as follows:

1. The onsets of cardiac cycles are detected by QRS detection techniques. The QRS complex is the combination of three waves observed within electrocardiograph traces. A separate ECG recording is necessary for this purpose.
2. An artifact template is formed by averaging across multiple cardiac cycles.

3. Temporal principal components are calculated for all time-locked occurrences of the artifact using singular value decomposition. This generates an optimal basis set (OBS), comprising principal components that explain the BCG variance over time [56].
4. The OBS is then regressed out from each occurrence of BCG artifacts.

Blind-Source Separation of BCG Artifacts

BCG artifacts can also be removed by using blind-source separation techniques based on ICA [40, 75]. ICA unmixes EEG data into source components, some of which will be noise and others which will be the brain signal of interest. Due to ICA's ability to identify noise sources, the noise sources can simply be regressed out in the time-domain from raw EEG data, resulting in cleaner EEG signals. Several other approaches have been used for ICA-based removal of BCG artifacts, including: (1) temporal ICA and (2) hybrid AAS + ICA methods [7, 65]. In the temporal ICA approach, the ICA algorithm is applied on continuous EEG data, resulting in component time-courses corresponding to noise and the brain signal [40]. In this approach, noise components must be identified accurately to be able to remove them effectively. However, objective and validated identification of BCG components is difficult and remains a major challenge. To identify the noise components, methods based on correlation with ECG signals are often used [40]. Other more advanced methods which detect auto-correlation in each IC for peaks associated with the cardiac cycle or use spectral analysis of components have also been proposed and used [7, 40, 73].

Hybrid AAS + ICA approaches make use of advantages associated with both AAS- and ICA-based methods [73, 76]. This approach first computes optimal basis sets from artifact templates generated from cardiac-cycle-locked EEG data. Most of the BCG artifacts are removed using this approach. ICA is then used to remove residual BCG artifacts [75].

Hardware-Based Approaches

Hardware-based approaches can also be used to remove BCG artifacts from the EEG data [58, 69, 72, 77]. This approach uses an extra sensor to monitor cardiac-pulse-related motion and head movements during concurrent EEG-fMRI acquisitions. Carbon-wire loops have also been proposed to record and remove BCG artifacts from EEG data [71, 72]. Motion and BCG artifacts can also be recorded by simply insulating a few electrodes in the EEG cap and measuring the signal on these electrodes with respect to the reference electrode. These artifact signals are then regressed out of the EEG data. The BCG signal can also be estimated from a layer of electrodes added to a standard EEG cap.

7 Analysis of Simultaneously Recorded fMRI and EEG Data

Methods for analyzing simultaneous fMRI-EEG can be divided into model-driven and data-driven techniques [7, 78] (Fig. 5). Model-driven techniques aim to fit EEG-derived brain signals to fMRI data (EEG-informed fMRI) or, conversely, fMRI-derived brain signals to EEG data (fMRI-informed EEG), thus improving the spatiotemporal resolution with which neural processes can be interrogated [7]. In contrast, data-driven techniques aim to integrate fMRI and EEG data with a minimum of prior assumptions regarding underlying neural activity [79, 80].

7.1 Model-Driven Techniques

Model-driven techniques use linear or nonlinear models to combine temporal, spectral, or spatiotemporal activity inherent in EEG and fMRI. This approach has been used to investigate fMRI correlates of both oscillatory and event-related neuronal activity in EEG data, at the individual-subject level [4, 5, 10, 11, 14, 33,

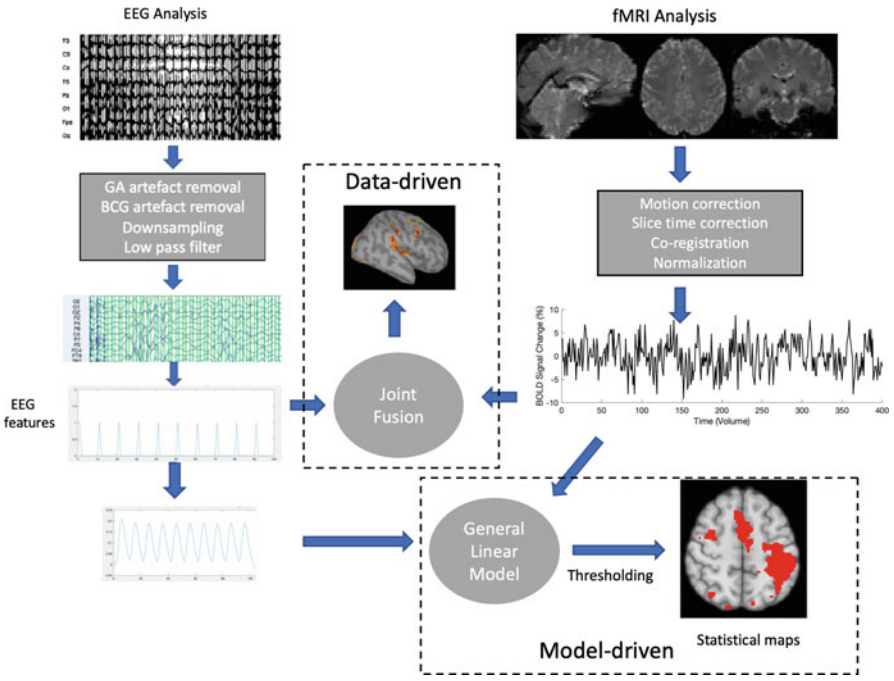

Fig. 5 A high-level overview of the process used in the analyses of simultaneous fMRI and EEG data. Raw EEG data is processed to identify events of interest. The events are convolved with a typical hemodynamic response and fitted to the fMRI data

62, 81–83]. To investigate spatial fMRI correlates of oscillatory EEG activity in a specific frequency band (e.g., 7–13 Hz alpha), the activity is identified visually (using subjective knowledge), or using time-frequency analysis and labeled as events of interests [5, 9]. Moving window time-series of EEG power in a specific frequency band can be used as a regressor in a general linear model (GLM) analysis where fMRI time-series is an outcome variable and EEG power is a predictor. In an event-related design, distinct features of the EEG can be used, such as EEG coherence, frequency-specific EEG power, and ERP amplitude or latencies [84, 85]. These features are then used in an event-related or epoch model to model the transient/phasic effect of neural activity on fMRI. The design is then convolved with the hemodynamic response function to model the temporal fluctuations in fMRI associated with EEG changes. The basic assumption underlying this approach is that the temporal fluctuations in EEG features covary with fluctuations in fMRI.

7.2 Data-Driven Techniques

Data-driven techniques can fuse fMRI and EEG data to provide a high-resolution map of brain function [86, 87]. These approaches rely on a minimum of neurophysiological assumptions regarding neurovascular coupling and neural signal flow in the brain. Data-driven techniques can be used to analyze fMRI data without a prior model. This is particularly important in some behavior-driven experiments, such as resting state, in which there is no explicit model for the data. However, the usefulness of data-driven techniques is limited by the fact that EEG signal is largely cortical in nature. The most commonly used data-driven techniques are independent component analysis (ICA) and clustering.

Fusion Using Independent Component Analysis ICA is used in fMRI to identify spatially and/or temporally independent structures in the data [88]. Most applications of ICA to fMRI seek components that are maximally independent spatially. ICA assumes that the observed signal is a linear combination of independent sources and uses higher-order statistics to identify them. Joint ICA has been used to extract spatiotemporal patterns of BOLD signals related to motor sequence learning [89], object recognition [90], and the resting-state network [91]. For example, a joint ICA-based approach developed to fuse multimodal EEG and fMRI data [86, 87] can combine single-trial EEG and fMRI without prior information of ERP amplitude or phase. In this approach, single-trial EEG responses and fMRI responses can be merged into a single matrix and subjected to a joint spatiotemporal decomposition [87]. Another approach applies ICA sources to fuse EEG + fMRI data [92]. This method also combines the constrained and lag-based signal decomposition approaches to demonstrate variable lag structures between electrophysiological and BOLD signals [92].

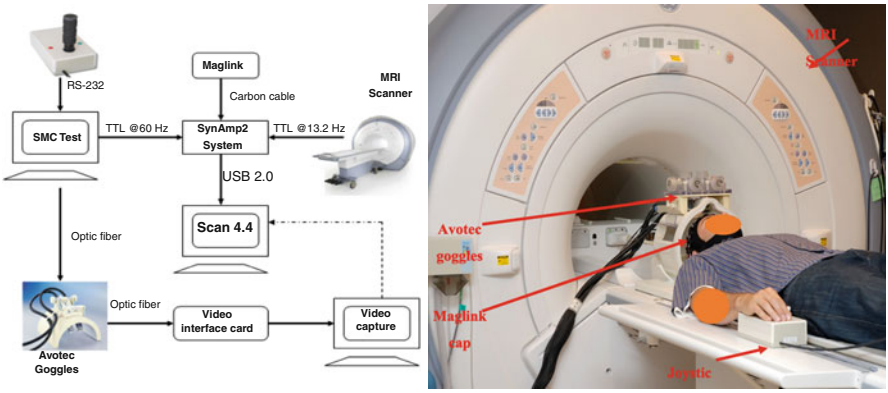

Fig. 6 Schematic of the simultaneous recording system. The EEG system, joystick, eye-video recording system, and the MRI scanner were synchronized via triggers sent to the EEG system. The right tab shows the subject prepared for an MRI session. The subject is holding the finger-based joystick, and is fitted with an EEG cap

8 Experimental Techniques for Simultaneous fMRI and EEG

Simultaneous fMRI-EEG has been used extensively as a tool to answer questions related to brain function, with exponential growth in its use in recent years [3, 14, 43, 58, 83]. Most of these studies used highly controlled experimental manipulations, comparing fMRI and/or EEG activity during controlled stimuli presentations. However, the need to study the brain without any experimental input (e.g., spontaneous behavior) is also been well recognized. Consequently, simultaneous fMRI-EEG studies of sleep and other real-world phenomena have emerged over recent years [5, 9, 34, 51, 52, 93–95]. The following provides an overview of various experimental approaches to the study of the human brain using EEG + fMRI (Fig. 6).

8.1 Controlled Experiments

Controlled experiments are conducted by presenting carefully-timed experimental stimuli of pre-defined duration during simultaneous fMRI-EEG studies. The type of stimuli and experimental conditions depend on the research questions being investigated, with experiments requiring at least two types of conditions: baseline and task conditions. This is required because the fMRI BOLD signal is not an absolute measure of neuronal activity. Hence, all studies must incorporate the ability to statistically contrast the neuronal activity of interest with a suitable background (i.e.,

baseline) condition [96]. Most simultaneous fMRI-EEG use event-related designs, in which experimental conditions are presented as short-duration events in arbitrary sequences eliminating potential confounds, such as habituation, anticipation, set, or other strategy effects [97]. It is assumed that each event generates neuronal activity resulting in a transient BOLD and EEG response. By comparing the simultaneous fMRI-EEG activity between different types of events, research questions on changes in neural activity as a function of independent variables can be answered. Event-related designs also allow for analyses of individual responses to trials, providing the means to identify neural correlates of behavioral responses, such as errors in reaction time paradigms [98, 99].

Experiments in which stimuli of the same type are presented in blocks are known as blocked-design studies. This model assumes that steady-state neuronal activity and hemodynamics are attained within each block [100]. Mixed designs combine elements of both event-related and block-design approaches [13, 101]. Similar to block design, there are control blocks and task blocks. But, in contrast to block design, in each task block trials are presented with different intervals between them, as in event-related designs. This method allows estimation of the temporal profile of activity related to each trial along with the estimation of sustained activity throughout a task block.

8.2 Behavior-Driven Experiments

In behavior-driven experiments , the simultaneous fMRI-EEG is used to investigate variations in spontaneous behavior. A simple behavior-driven experiment is a resting-state experiment in which subjects lie inside an MRI scanner doing nothing other than static visual fixation, and the EEG and BOLD fMRI activity related to the resting behavior is measured [102]. From this viewpoint, spontaneous activity in the resting state can reveal the functional organization of the brain.

The second type of behavior-driven fMRI studies are those that investigate the BOLD and EEG signal associated with spontaneous fluctuations in physiological activity. Generally, these studies record physiological activities such as galvanic skin response, EEG, and ECG during fMRI scanning, in which changes are identified post-hoc and correlated with the BOLD response [9, 10, 93, 103].

Despite the growth of behavior-driven studies, each new behavior-driven study poses a new challenge, because the lack of discrete stimuli means that standard experimental designs and analyses cannot be used. Moreover, “dynamic, continuous stimuli can evoke both transient and sustained responses within the same brain region or in different brain regions simultaneously, making data interpretation difficult” [104]. The unconstrained nature of eye movements, multiple features in any given scene, and the lack of a specific task can give rise to ambiguity about what subjects were attending to or thinking about during the experience [104]. Thus, it is important to record as many behavioral and physiological characteristics such as eye-movement, eye-video, skin conductance, ECG, and EEG during behavior-driven experiments so that any variability in BOLD signal fluctuations due to these factors can be accounted for.

9 Conclusions

Simultaneous fMRI-EEG is a state-of-the-art brain imaging technique which can be used to better understand the spatiotemporal dynamics of human brain activity. This modality provides an ability to investigate the functioning of the brain networks and can provide information on the sources of electrical activity in the brain with a high temporal and spatial resolution. However, several technical challenges should be taken into account before planning for simultaneous fMRI-EEG studies. Choice of pre-processing strategy depends upon the type of hardware and amount of noise in the data. However, the field still lacks an optimal integrated and standardized analysis plan that is reliable and replicable across studies. Studies are needed to standardize the data acquisition, pre-processing, and analysis pipelines for EEG + fMRI studies.

This notwithstanding, the field of cognitive neuroscience has benefited immensely from the availability of this technique.

References

1. Ives, J.R., et al.: Monitoring the patient's EEG during echo planar MRI. Electroencephalogr. Clin. Neurophysiol. **87**(6), 417–420 (1993)
2. Goldman, R.I., et al.: Acquiring simultaneous EEG and functional MRI. Clin. Neurophysiol. **111**(11), 1974–1980 (2000)
3. Abreu, R., Leal, A., Figueiredo, P.: EEG-informed fMRI: a review of data analysis methods. Front. Hum. Neurosci. **12**, 29 (2018)
4. Simoes, M., et al.: Correlated alpha activity with the facial expression processing network in a simultaneous EEG-fMRI experiment. Conf. Proc. IEEE Eng. Med. Biol. Soc. **2017**, 2562–2565 (2017)
5. Poudel, G.R., et al.: Losing the struggle to stay awake: divergent thalamic and cortical activity during microsleeps. Hum. Brain Mapp. **35**(1), 257–269 (2014)
6. Noth, U., et al.: Simultaneous electroencephalography-functional MRI at 3 t: an analysis of safety risks imposed by performing anatomical reference scans with the EEG equipment in place. J. Magn. Reson. Imaging. **35**(3), 561–571 (2012)
7. Huster, R.J., et al.: Methods for simultaneous EEG-fMRI: an introductory review. J. Neurosci. **32**(18), 6053–6060 (2012)
8. Michels, L., et al.: Simultaneous EEG-fMRI during a working memory task: modulations in low and high frequency bands. PLoS One. **5**(4), e10298 (2010)
9. Kaufmann, C., et al.: Brain activation and hypothalamic functional connectivity during human non-rapid eye movement sleep: an EEG/fMRI study. Brain. **129**(Pt 3), 655–667 (2006)
10. Laufs, H., et al.: EEG-correlated fMRI of human alpha activity. NeuroImage. **19**(4), 1463–1476 (2003)
11. Goldman, R.I., et al.: Simultaneous EEG and fMRI of the alpha rhythm. NeuroReport. **13**(18), 2487–2492 (2002)
12. Liu, Z.M., He, B.: FMRI-EEG integrated cortical source imaging by use of time-variant spatial constraints. NeuroImage. **39**(3), 1198–1214 (2008)
13. Poudel, G.R., Innes, C.R.H., Jones, R.D.: Distinct neural correlates of time-on-task and transient errors during a visuomotor tracking task after sleep restriction. NeuroImage. **77**, 105–113 (2013)
14. Poudel, G.R., Innes, C.R.H., Jones, R.D.: Temporal evolution of neural activity and connectivity during microsleeps when rested and following sleep restriction. NeuroImage. **174**, 263–273 (2018)

15. Ogawa, S., et al.: Brain magnetic resonance imaging with contrast dependent on blood oxygenation. Proc. Natl. Acad. Sci. **87**, 9868–9872 (1990)
16. Arthurs, O.J., Boniface, S.: How well do we understand the neural origins of the fMRI bold signal? Trends Neurosci. **25**(3), 169–169 (2002)
17. Salek-Haddadi, A., et al.: Studying spontaneous EEG activity with fMRI. Brain Res. Rev. **43**(1), 110–133 (2003)
18. Buxton, R.B., Wong, E.C., Frank, L.R.: Dynamics of blood flow and oxygenation changes during brain activation; the balloon model. Magn. Reson. Med. **39**, 855–864 (1998)
19. Logothetis, N.K., et al.: Neurophysiological investigation of the basis of the fMRI signal. Nature. **412**(6843), 150–157 (2001)
20. Lindquist, M.A., et al.: Modeling the hemodynamic response function in fMRI: efficiency, bias and mis-modeling. NeuroImage. **45**(1 Suppl), S187–S198 (2009)
21. Menon, R.S., et al.: BOLD based functional MRI at 4 Tesla includes a capillary bed contribution: echo-planar imaging correlates with previous optical imaging using intrinsic signals. Magn. Reson. Med. **33**(3), 453 (1995)
22. Hu, X., Yacoub, E.: The story of the initial dip in fMRI. NeuroImage. **62**(2), 1103–1108 (2012)
23. Gras, V., et al.: Optimizing bold sensitivity in the 7t human connectome project resting-state fMRI protocol using plug-and-play parallel transmission. NeuroImage. **195**, 1–10 (2019)
24. Kim, S.-G., Ogawa, S.: Insights into new techniques for high resolution functional MRI. Curr. Opin. Neurobiol. **12**(5), 607–615 (2002)
25. Kashyap, S., et al.: Resolving laminar activation in human v1 using ultra-high spatial resolution fMRI at 7t. Sci. Rep. **8**, 17063 (2018)
26. Tsuchida, T.N., et al.: American clinical neurophysiology society: EEG guidelines introduction. J. Clin. Neurophysiol. **33**(4), 301–302 (2016)
27. Kirschstein, T., Kohling, R.: What is the source of the EEG? Clin. EEG Neurosci. **40**(3), 146–149 (2009)
28. Buzsaki, G., Anastassiou, C.A., Koch, C.: The origin of extracellular fields and currents–EEG, ECOG, LFP and spikes. Nat. Rev. Neurosci. **13**(6), 407–420 (2012)
29. Cajochen, C., Foy, R., Dijk, D.J.: Frontal predominance of a relative increase in sleep delta and theta EEG activity after sleep loss in humans. Sleep Res. Online. **2**(3), 65–69 (1999)
30. Accolla, E.A., et al.: Clinical correlates of frontal intermittent rhythmic delta activity (FIRDA). Clin. Neurophysiol. **122**(1), 27–31 (2011)
31. Makeig, S., Jung, T.P., Sejnowski, T.J.: Awareness during drowsiness: dynamics and electrophysiological correlates. Can. J. Exp. Psychol. **54**(4), 266–273 (2000)
32. Makeig, S., Jung, T.P.: Tonic, phasic, and transient EEG correlates of auditory awareness in drowsiness. Brain Res. Cogn. Brain Res. **4**(1), 15–25 (1996)
33. Brueggen, K., et al.: Early changes in alpha band power and dmn bold activity in Alzheimer's disease: a simultaneous resting state EEG-fMRI study. Front. Aging Neurosci. **9**, 319 (2017)
34. Dang-Vu, T.T., et al.: Spontaneous neural activity during human slow wave sleep. Proc. Natl. Acad. Sci. U. S. A. **105**(39), 15160–15165 (2008)
35. Liu, Y., et al.: Top-down modulation of neural activity in anticipatory visual attention: control mechanisms revealed by simultaneous EEG-fMRI. Cereb. Cortex. **26**(2), 517–529 (2016)
36. Mullinger, K., et al.: Effects of simultaneous EEG recording on MRI data quality at 1.5, 3 and 7 tesla. Int. J. Psychophysiol. **67**(3), 178–188 (2008)
37. Hawsawi, H.B., Carmichael, D.W., Lemieux, L.: Safety of simultaneous scalp or intracranial EEG during MRI: a review. Front. Phys. **5**, 42 (2017)
38. Lemieux, L., et al.: Recording of EEG during fMRI experiments: patient safety. Magn. Reson. Med. **38**(6), 943–952 (1997)
39. Salek-Haddadi, A., et al.: EEG quality during simultaneous functional MRI of interictal epileptiform discharges. Magn. Reson. Imaging. **21**(10), 1159–1166 (2003)
40. Srivastava, G., et al.: Ica-based procedures for removing ballistocardiogram artifacts from EEG data acquired in the MRI scanner. NeuroImage. **24**(1), 50–60 (2005)

41. Jonmohamadi, Y., et al.: Source-space ICA for EEG source separation, localization, and time-course reconstruction. NeuroImage. **101**, 720–737 (2014)
42. Toppi, J., et al.: Time-varying effective connectivity of the cortical neuroelectric activity associated with behavioural microsleeps. NeuroImage. **124**(Pt A), 421–432 (2016)
43. Bayer, M., Rubens, M.T., Johnstone, T.: Simultaneous EEG-fMRI reveals attention-dependent coupling of early face processing with a distributed cortical network. Biol. Psychol. **132**, 133–142 (2018)
44. Bonmassar, G., et al.: Spatiotemporal brain imaging of visual-evoked activity using interleaved EEG and fMRI recordings. NeuroImage. **13**(6), 1035–1043 (2001)
45. Portas, C.M., et al.: Auditory processing across the sleep-wake cycle: simultaneous EEG and fMRI monitoring in humans. Neuron. **28**(3), 991–999 (2000)
46. Menon, V., Crottaz-Herbette, S.: Combined EEG and fMRI studies of human brain function. Neuroimaging. **66**(Pt A), 291 (2005)
47. Hall, D.A., et al.: "Sparse" temporal sampling in auditory fMRI. Hum. Brain Mapp. **7**(3), 213–223 (1999)
48. Schwarzbauer, C., et al.: Interleaved silent steady state (ISSS) imaging: a new sparse imaging method applied to auditory fMRI. NeuroImage. **29**(3), 774–782 (2006)
49. Poudel, G.R., et al.: Neural correlates of decision-making during a Bayesian choice task. NeuroReport. **28**(4), 193–199 (2017)
50. McGlashan, E.M., et al.: Imaging individual differences in the response of the human suprachiasmatic area to light. Front. Neurol. **9**, 1022 (2018)
51. Schabus, M., et al.: Neural correlates of sleep spindles as revealed by simultaneous electroencephalography (EEG) and functional magnetic resonance imaging (fMRI). J. Sleep Res. **15**, 50–51 (2006)
52. Fang, L., et al.: Simultaneous EEG-fMRI reveals spindle-related neural correlates of human intellectual abilities during NREM sleep. Sleep Med. **40**, E99–E99 (2017)
53. Mullinger, K.J., Castellone, P., Bowtell, R.: Best current practice for obtaining high quality EEG data during simultaneous fMRI. J. Vis. Exp. (76) (2013)
54. Allen, P.J., Josephs, O., Turner, R.: A method for removing imaging artifact from continuous EEG recorded during functional MRI. NeuroImage. **12**(2), 230–239 (2000)
55. Negishi, M., et al.: Removal of time-varying gradient artifacts from EEG data acquired during continuous fMRI. Clin. Neurophysiol. **115**(9), 2181–2192 (2004)
56. Niazy, R.K., et al.: Removal of fMRI environment artifacts from EEG data using optimal basis sets. NeuroImage. **28**(3), 720–737 (2005)
57. Ritter, P., Villringer, A.: Simultaneous EEG-fMRI. Neurosci. Biobehav. Rev. **30**(6), 823–838 (2006)
58. Chowdhury, M.E.H., et al.: Simultaneous EEG-fMRI: evaluating the effect of the EEG cap-cabling configuration on the gradient artifact. Front. Neurosci. **13**, 690 (2019)
59. Cunningham, C.J.B., et al.: Simultaneous EEG-fMRI in human epilepsy. Can. J. Neurol. Sci. **35**(4), 420–435 (2008)
60. Sartori, E., et al.: Gradient artifact removal in co-registration EEG/fMRI. World Congress on Medical Physics and Biomedical Engineering, Vol 25, Pt 4: Image Processing, Biosignal Processing, Modelling and Simulation. Biomechanics. **25**, 1143–1146 (2010)
61. Freyer, F., et al.: Ultrahigh-frequency EEG during fMRI: pushing the limits of imaging-artifact correction. NeuroImage. **48**(1), 94–108 (2009)
62. de Munck, J.C., et al.: The hemodynamic response of the alpha rhythm: an EEG/fMRI study. NeuroImage. **35**(3), 1142–1151 (2007)
63. Moosmann, M., et al.: Realignment parameter-informed artefact correction for simultaneous EEG-fMRI recordings. NeuroImage. **45**(4), 1144–1150 (2009)
64. Ryali, S., et al.: Development, validation, and comparison of ICA-based gradient artifact reduction algorithms for simultaneous EEG-spiral in/out and echo-planar fMRI recordings. NeuroImage. **48**(2), 348–361 (2009)
65. Mantini, D., et al.: Complete artifact removal for EEG recorded during continuous fMRI using independent component analysis. NeuroImage. **34**(2), 598–607 (2007)

66. Chechile, R.A.: Independent component analysis: a tutorial introduction. J. Math. Psychol. **49**(5), 426–426 (2005)
67. Islam, M.K., Rastegarnia, A., Yang, Z.: Methods for artifact detection and removal from scalp EEG: a review. Clin. Neurophysiol. **46**(4-5), 287–305 (2016)
68. Acharjee, P.P., et al.: Independent vector analysis for gradient artifact removal in concurrent EEG-fMRI data. IEEE Trans. Biomed. Eng. **62**(7), 1750–1758 (2015)
69. Chowdhury, M.E.H., et al.: Reference layer artefact subtraction (RLAS): a novel method of minimizing EEG artefacts during simultaneous fMRI (vol 84, pg 307, 2014). NeuroImage. **98**, 547–547 (2014)
70. Maziero, D., et al.: Towards motion insensitive EEG-fMRI: correcting motion-induced voltages and gradient artefact instability in EEG using an fMRI prospective motion correction (PMC) system. NeuroImage. **138**, 13–27 (2016)
71. van der Meer, J.N., et al.: Carbon-wire loop based artifact correction outperforms post-processing EEG/fMRI corrections-a validation of a real-time simultaneous EEG/fMRI correction method. NeuroImage. **125**, 880–894 (2016)
72. Abbott, D.E., et al.: Constructing carbon fiber motion-detection loops for simultaneous EEG-fMRI. Front. Neurol. **5**, 260 (2015)
73. Debener, S., et al.: Properties of the ballistocardiogram artefact as revealed by EEG recordings at 1.5, 3 and 7 t static magnetic field strength. Int. J. Psychophysiol. **67**(3), 189–199 (2008)
74. Grouiller, F., et al.: A comparative study of different artefact removal algorithms for EEG signals acquired during functional MRI. NeuroImage. **38**(1), 124–137 (2007)
75. Wang, K., et al.: Clustering-constrained ICA for ballistocardiogram artifacts removal in simultaneous EEG-fMRI. Front. Neurosci. **12**, 59 (2018)
76. Mayeli, A., et al.: Real-time EEG artifact correction during fMRI using ICA. J. Neurosci. Methods. **274**, 27–37 (2016)
77. Masterton, R.A.J., et al.: Measurement and reduction of motion and ballistocardiogram artefacts from simultaneous EEG and fMRI recordings. NeuroImage. **37**(1), 202–211 (2007)
78. Valdes-Sosa, P.A., et al.: Model driven EEG/fMRI fusion of brain oscillations. Hum. Brain Mapp. **30**(9), 2701–2721 (2009)
79. Dong, L., et al.: Simultaneous EEG-fMRI: trial level spatio-temporal fusion for hierarchically reliable information discovery. NeuroImage. **99**, 28–41 (2014)
80. Daunizeau, J., et al.: Symmetrical event-related EEG/fMRI information fusion in a variational Bayesian framework. NeuroImage. **36**(1), 69–87 (2007)
81. Singh, M., Patel, P., Al-Dayeh, L.: FMRI of brain activity during alpha rhythm. International Society for Magnetic Resonance in Medicine, Concord, CA (1998)
82. Omata, K., et al.: Spontaneous slow fluctuation of EEG alpha rhythm reflects activity in deep-brain structures: a simultaneous EEG-fMRI study. PLoS One. **8**(6), e66869 (2013)
83. Ragazzoni, A., et al.: "Hit the missing stimulus". A simultaneous EEG-fMRI study to localize the generators of endogenous ERPs in an omitted target paradigm. Sci. Rep. **9**, 3684 (2019)
84. Scheeringa, R., et al.: Frontal theta EEG activity correlates negatively with the default mode network in resting state. Int. J. Psychophysiol. **67**(3), 242–251 (2008)
85. Jann, K., et al.: Bold correlates of EEG alpha phase-locking and the fMRI default mode network. NeuroImage. **45**(3), 903–916 (2009)
86. Calhoun, V.D., et al.: Neuronal chronometry of target detection: fusion of hemodynamic and event-related potential data. NeuroImage. **30**(2), 544–553 (2006)
87. Moosmann, M., et al.: Joint independent component analysis for simultaneous EEG-fMRI: principle and simulation. Int. J. Psychophysiol. **67**(3), 212–221 (2008)
88. McKeown, M.J., et al.: Analysis of fMRI data by blind separation into independent spatial components. Hum. Brain Mapp. **6**(3), 160–188 (1998)
89. Kincses, Z.T., et al.: Model-free characterization of brain functional networks for motor sequence learning using fMRI. NeuroImage. **39**(4), 1950–1958 (2008)
90. Habas, C., Cabanis, E.A.: Dissociation of the neural networks recruited during a haptic object-recognition task: complementary results with a tensorial independent component analysis. Am. J. Neuroradiol. **29**(9), 1715–1721 (2008)

91. Damoiseaux, J.S., et al.: Consistent resting-state networks across healthy subjects. Proc. Natl. Acad. Sci. U. S. A. **103**(37), 13848–13853 (2006)
92. Jonmohamadi, Y., et al.: Constrained temporal parallel decomposition for EEG-fMRI fusion. J. Neural Eng. **16**(1), 016017 (2019)
93. Laufs, H., et al.: Where the BOLD signal goes when alpha EEG leaves. NeuroImage. **31**, 1408 (2006)
94. Spiers, H.J., Maguire, E.A.: Neural substrates of driving behaviour. NeuroImage. **36**(1), 245–255 (2007)
95. Hutchison, K., et al.: Cortical activation can be visualized during sleep using simultaneous EEG-fMRI. Sleep. **30**, A36–A37 (2007)
96. Culham, J.C.: Functional neuroimaging: experimental design and analysis. In: Handbook of Functional Neuroimaging of Cognition, pp. 53–82. MIT Press, Cambridge, MA (2006)
97. Dale, A.M.: Optimal experimental design for event-related fMRI. Hum. Brain Mapp. **8**(2-3), 109–114 (1999)
98. Hopfinger, J.B., Buonocore, M.H., Mangun, G.R.: The neural mechanisms of top-down attentional control. Nat. Neurosci. **3**, 284–291 (2000)
99. Weissman, D., et al.: The neural bases of momentary lapses in attention. Nat. Neurosci. **9**, 971–978 (2006)
100. Mechelli, A., et al.: Comparing event-related and epoch analysis in blocked design fMRI. NeuroImage. **18**(3), 806–810 (2003)
101. Visscher, K.M., et al.: Mixed blocked/event-related designs separate transient and sustained activity in fMRI. NeuroImage. **19**(4), 1694–1708 (2003)
102. Fox, M.D., et al.: The human brain is intrinsically organized into dynamic, anticorrelated functional networks. Proc. Natl. Acad. Sci. **102**(27), 9673–9678 (2005)
103. Critchley, H.D., et al.: Neural activity relating to generation and representation of galvanic skin conductance responses: a functional magnetic resonance imaging study. J. Neurosci. **20**(8), 3033 (2000)
104. Spiers, H., Maguire, E.: Decoding human brain activity during real-world experiences. Trends Cogn. Sci. **11**(8), 356–365 (2007)